Journal of Soil Science and Plant Nutrition
https://doi.org/10.1007/s42729-025-02509-6

ORIGINAL PAPER

Biochar Application to Recover Degraded Soils: Comparison of Different Biomass Sources Assessed by Soil Physical Quality and Maize Growth

Tiago da Costa Dantas Moniz[1] · João Marcos Rodrigues dos Santos[1] · Gilvanete da Silva Henrique[1] · Francisco Luan Almeida Barbosa[1] · João Ivo Rodrigues de Sousa[1] · Ícaro Vasconcelos do Nascimento[1] · Alexandre dos Santos Queiroz[1] · Carlos Tadeu dos Santos Dias[2] · Maria Vitória Ricarte Gonçalves[1] · Mirian Cristina Gomes Costa[1] · Helon Hébano de Freitas Sousa[1] · Francisca Gleiciane da Silva[1] · Laís Gomes Fregolente[3] · Odair Pastor Ferreira[4] · Antônio Gomes de Souza Filho[5] · Rafael Santiago da Costa[6] · Jaedson Cláudio Anunciato Mota[1]

Received: 12 December 2024 / Accepted: 28 May 2025

Abstract

Biochar application is strategic to improve soil quality and productivity. However, the effects of biochar produced from sewage sludge with cashew pruning biomass; and cashew bagasse on the physical attributes of degraded soils in arid regions remain unclear. The hypotheses were: (1) biochars from the co-pyrolysis of sewage sludge and cashew pruning (SSPB) and cashew bagasse (CBB) improve the physical quality of degraded soil and maize growth; (2) SSPB, richer in nutrients, facilitates better maize growth compared to CBB; (3) for each biochar, there is an optimal rate to improve soil physical quality and maize growth. We collected samples in the 0–10 cm layer of a Planosol from a desertification nucleus. The experiment was conducted in a greenhouse with a completely randomized design in a factorial scheme $2 \times 4 + 1$ (two biochars: SSPB and CBB; four doses: 5, 10, 20, and 40 Mg ha^{-1}; and a control), totaling 36 experimental units. Water demand, plant development, and soil physical attributes were assessed. During incubation, SSPB at 5 and 10 Mg ha^{-1} reduced available water capacity (AWC) by 25% compared to the control. In post-cultivation, SSPB reduced penetration resistance and increased aggregate stability. CBB increased AWC by 30% and reduced water demand by 40% at 9 Mg ha^{-1}. SSPB reduced bulk density by 4% at 22.6 Mg ha^{-1}. SSPB improved soil physical quality significantly, while CBB optimized water use efficiency. Recommended doses are 20–25 Mg ha^{-1} for SSPB and 9 Mg ha^{-1} for CBB.

Keywords Soil conditioners · Soil quality · Carbonaceous material · Degraded areas

✉ Ícaro Vasconcelos do Nascimento
icaro_agro@hotmail.com

[1] Soil Science Department, Federal University of Ceará (UFC), 2977, Av. Mister Hull, Campus do Pici, 60356-001 Fortaleza, CE, Brazil

[2] Department of Statistics, Federal University of Ceará (UFC), Campus do Pici, 60455-900 Fortaleza, CE, Brazil

[3] Brazilian Nanotechnology National Laboratory, Brazilian Center for Research in Energy and Materials, 10000, Street Giuseppe Máximo Scolfaro - Campinas High Technology Pole II, 13083-100 Campinas, SP, Brazil

[4] Department of Chemistry, Estadual University of Londrina (UEL), 86065-970 Londrina, PR, Brazil

[5] Department of Physics, Federal University of Ceará (UFC), Campus do Pici, 60455-900 Fortaleza, CE, Brazil

[6] Ceará Water and Sewage Company, Vila União, 60.422-901 Fortaleza, CE, Brazil

Published online: 09 June 2025

1 Introduction

Soil has well-defined ecosystem functions, such as providing physical support for plants and acting as a reservoir of essential nutrients, water, and oxygen for developing plants and animals (Koorneef et al. 2024). However, such functions can be compromised by the degradation process, which can occur not only due to adverse climatic conditions but also due to human activities, particularly improper land use. In drylands, environmental conditions make the soil more susceptible to degradation. Inadequate management of this resource, such as overgrazing, leads to the loss of vegetation and depletion of soil water resources, ultimately compromising the land's biological potential and accelerating desertification (Silva et al. 2023).

A strategy to enhance the physical-hydrological attributes of soil is the use of conditioners. Biochar, a soil conditioner gaining prominence, can improve the soil's physical, chemical, and biological properties, optimizing conditions for plant growth when applied to the soil. Notably, these products promote the formation of stable aggregates, which contribute to improving soil structure by increasing porosity and permeability to water and air flows. Additionally, they can enhance the soil's water retention capacity (Costa et al. 2022). This is particularly important in dry lands, as plants can access water stored in the soil pores.

The pyrolysis process generates forms of organic carbon in aromatic ring structures, which play a crucial role in the properties of biochar (Kloss et al. 2012). The composition of the biomass used as raw material for pyrolysis directly influences the formation of these aromatic structures, affecting the physical and chemical attributes of the carbonaceous material, such as porosity, specific surface area, pH, and cation exchange capacity (Kumar et al. 2020).

Co-pyrolysis refers to biochar produced from the pyrolysis of biomass mixed with another biomass, aiming to improve the product's physical and chemical properties (Goldan et al. 2022). Research is being conducted using the co-pyrolysis of lignocellulosic biomass with the addition of another biomass to absorb and immobilize heavy metals (Li et al. 2021). The International Biochar Initiative (IBI) defines maximum allowable heavy metal concentrations in biochar for agricultural applications, including lead (300 mg kg^{-1}), cadmium (39 mg kg^{-1}), chromium (1200 mg kg^{-1}), copper (6000 mg kg^{-1}), nickel (420 mg kg^{-1}), zinc (7400 mg kg^{-1}), and mercury (17 mg kg^{-1}), to mitigate soil contamination risks and ensure crop safety (IBI, 2015). Thus, the co-pyrolysis of sewage sludge with lignocellulosic biomass presents a promising alternative to produce a soil conditioner with safe and advantageous properties, aligning with IBI thresholds.

Biochar amendment has been extensively studied for its potential to enhance various soil physical properties. Research indicates that biochar application can significantly improve soil physical quality, including increasing water retention (by 4% to 130%) and porosity (by 14% to 64%), while simultaneously reducing bulk density (by 3% to 31%), thereby promoting overall soil health (Blanco-Canqui 2017). Additionally, biochar derived from specific feedstocks, such as cashew residue, has been shown to decrease maximum shear stress by 22.3%, further contributing to improved soil structure (Nascimento et al. 2024).

Co-pyrolysis, a promising thermochemical conversion technology, involves the simultaneous pyrolysis of two or more different biomass feedstocks to produce biochar with tailored properties (Fakayode et al. 2020). The characteristics of the resulting biochar are highly dependent on the pyrolysis parameters employed, such as temperature ramping rates and gas flow, as well as the specific biomass combinations used, which can create synergistic effects that enhance porosity, surface area, and nutrient content compared to biochar produced from a single feedstock (Cao et al. 2024). Further research into optimizing co-pyrolysis parameters and exploring diverse biomass combinations is crucial for maximizing the benefits of this technology for soil amendment.

Studies have demonstrated that the application of biochar derived from the co-pyrolysis of sewage sludge supplemented with cashew tree residues and cashew bagasse contributed to the restoration of microbial biomass and enzymatic activity in degraded dryland areas (Barbosa et al. 2024). Another study revealed that the application of cashew bagasse biochar promoted improvements in the physical attributes of soils with cohesive characteristics (Nascimento et al. 2024).

Thus, this study addresses critical knowledge gaps in the literature. Despite extensive research on biochar applications, little is known about the specific effects of biochars derived from the co-pyrolysis of sewage sludge with cashew pruning and from cashew bagasse on soil degraded by overgrazing. Furthermore, while previous studies have often focused on field experiments, the controlled conditions of a greenhouse pot experiment allow for a more precise isolation of biochar effects on soil physical properties. By comparing different biochar treatments with a control, this research not only clarifies these underexplored mechanisms but also offers valuable insights for mitigating the environmental impacts of improper residue disposal and enhancing soil quality and crop productivity.

Based on the above, the following hypotheses were established: (1) biochars from the co-pyrolysis of sewage sludge and cashew pruning (SSPB) and cashew bagasse (CBB), due to their porous structure capable of storing water and being chemically active to promote particle aggregation, improve the

physical quality of degraded soil and maize growth; (2) SSPB, being richer in nutrients, facilitates better maize growth compared to CBB; (3) for each biochar, there is an optimal dose to improve the physical quality of soil undergoing degradation and the growth of maize.

In this context, the objective was to evaluate soil physical attributes (bulk and particle density, soil resistance to root penetration, water retention curve, tensile strength, and aggregate stability) and morphometric attributes of maize plants (height, culm diameter, and dry mass of aerial part, roots, and total).

2 Material and Methods

2.1 Collection of Soil Samples and Location.

We collected samples from the 0–10 cm layer in a Planosol (IUSS Working Group WRB 2022), degraded by overgrazing, in a desertification nucleus in the municipality of Irauçuba, Ceará (Fig. 1). This depth was chosen because the topsoil represents the most dynamic region of the soil, where most of the root activity, organic matter accumulation, and nutrient cycling occur (Tang et al. 2023). The soil was air-dried until it reached equilibrium with ambient moisture, then crushed with a roller and passed through a 2 mm mesh sieve to obtain air-dried fine earth. The soil attributes are presented in Table 1.

2.2 Experimental Design, Treatments, Biochars, and Assembly of Experimental Unit

A completely randomized design was used, arranged in a 2 $\times 4 + 1$ factorial scheme (two biochars: co-pyrolysis of sewage sludge and cashew pruning – SSPB and cashew bagasse – CBB; four doses: 5, 10, 20, and 40 Mg ha^{-1}, and a control

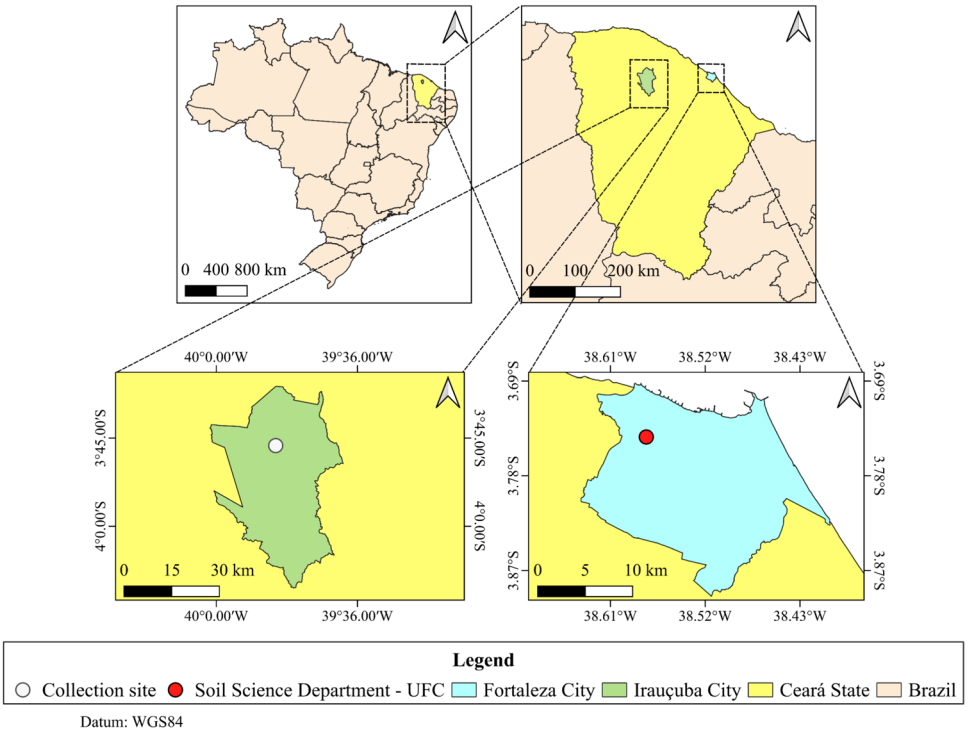

Fig. 1 A series of maps (WGS84) from Brazil to Ceará State, highlighting Fortaleza and the desertification nucleus of Irauçuba. The white circle indicates the soil-sampling site (0–10 cm depth; Planosol, IUSS Working Group WRB 2022) degraded by overgrazing; the red circle indicates the Soil Science Department, Federal University of Ceará (UFC), Fortaleza. Coordinates are shown in degrees

Table 1 Soil physical and chemical characterization

Layer (cm)			Sand			Silt			Clay			
0–10			76			17			7			
pH	CE	P	Ca^{2+}	Mg^{2+}	K^+	Na^+	Al^{3+}	$H^+ + Al^{3+}$	SB	T	V	C
H_2O	dS m^{-1}	Mg kg^{-1}	cmol$_c$ kg^{-1}								%	g kg^{-1}
5.1	0.03	8.44	6.97	0.46	0.09	0.08	0.54	2.52	7.52	10.04	74.90	6.07

P Extracted with Mehlich, *SB* Sum of bases, *T* Cation exchange capacity at pH 7.0, *V* Base saturation, and *C* Organic carbon extracted with potassium dichromate. Ca^{2+}, Mg^{2+}, and Al^{3+}: extracted with KCl; $H^+ + Al^{3+}$: extracted with calcium acetate

treatment), with four replications, totaling 36 experimental units.

Each experimental unit consisted of a Polyvinyl Chloride (PVC) column (20 cm in diameter, 50 cm in height), and in the biochar treatments, the conditioner was mixed with the soil homogenously before setting up the column.

During the assembly of the experimental units, a soil bulk density of 1.55 g cm^{-3} was used. According to Lima et al. (2024), bulk density in overgrazed areas where the soil was collected reaches a value of 1.85 g cm^{-3}; however, considering the incorporation of biochar with plowing and subsequent harrowing, the density is reduced, so a value of 1.55 g cm^{-3} was considered. Each column was filled with soil from the desertification nucleus with the biochar already incorporated according to the treatments studied in this work (for column assembly, soil passed through a 4 mm mesh sieve). While a constant soil bulk density of 1.55 g cm^{-3} was employed to ensure analytical consistency, it is important to note that soil bulk density inherently varies due to differences in soil composition, management practices, and climatic influences (Logsdon 2012), which may limit the direct extrapolation of these results to heterogeneous field conditions.

The biochar doses were determined based on Major (2010), who reported studies demonstrating positive effects with doses between 5 and 50 Mg ha^{-1}. Based on this, the initial dose was set at 5 Mg ha^{-1}, progressively doubling to 10, 20, and finally, 40 Mg ha^{-1}, keeping the doses below the upper limit mentioned in the literature.

For the SSPB treatment, sewage sludge from an upflow anaerobic sludge blanket reactor at a domestic wastewater treatment plant in Fortaleza, Ceará, Brazil, was co-pyrolyzed with cashew pruning residues at a 1:1 mass ratio to mitigate potential heavy metal contamination risks. For the CBB treatment, cashew bagasse was obtained from a cashew-producing farm in Aracati-CE, Brazil. Both biomasses were subjected to pyrolysis under a controlled atmosphere using a moderate flow of nitrogen as carrier gas. A heating rate of 10 °C min^{-1} was employed, and the target temperature of 500 °C was reached. Notably, the pyrolysis duration varied between the treatments: the co-pyrolysis process for SSPB lasted 1 h and 37 min, while for CBB, pyrolysis extended to 3 h and 10 min. After reaching the final temperature, the samples were allowed to cool under the continuous flow of nitrogen to prevent oxidation. The characterization of the resulting biochars is presented in Table 2.

Following standard fertilization and soil amendment recommendations for maize (*Zea mays* L.) in Ceará State (Fernandes et al., 1993), nutrient applications were tailored based on initial soil chemical characteristics (Table 1). Before sowing, basal fertilization was applied to each soil column, consisting of single superphosphate (4.436 mg), potassium chloride (421 mg), and urea (840 mg). Supplemental fertilization was subsequently provided in two equal applications at 25 and 45 days after emergence (DAE), each containing potassium chloride (210 mg) and urea (838 mg). Given the observed Ca:Mg imbalance (with calcium concentrations disproportionately higher than magnesium), soil correction was implemented through magnesium sulfate application to optimize the cation ratio.

2.3 Conduct of the Experiment

The experiment was conducted in a greenhouse located at coordinates 3°44′38.87"S and 38°34′31.34"W, in Fortaleza, Ceará, Brazil. The study was carried out with temperature maintained at 27 °C (reaching 35 °C during the hottest periods), and humidity control, maintained at 80%. After the columns were assembled and the biochar applied, the soil was maintained for 30 days to incubate the biochar with moisture between field capacity and a maximum consumption of 30% of the available water capacity (AWC). The incubation period was implemented to facilitate the development of structural modifications that could be detected using the soil quality indicators (Nascimento et al. 2024). AWC was calculated considering field capacity (matric potential of −10 kPa) and the permanent wilting point (matric potential of −1500 kPa). Soil water matric potential was monitored for irrigation management using tensiometers with a mercury manometer (one tensiometer in each column at a depth of 20 cm); distilled water was used to meet the water demand.

After biochar incubation, three maize seeds (variety BRS 2022) were sown per column, with subsequent thinning to maintain only the most vigorous plant. Irrigation management during the cultivation period was the same as described for the incubation period.

At the end of the experiment, samples were collected from the center of the 0–10 cm layer (i.e., between 2.5 and 7.5 cm) from each column. Both non-preserved samples (for particle density analysis) and preserved samples (using a volumetric ring of 5 cm in height and 5 cm in diameter) were taken to determine soil bulk density, soil–water retention curve, and soil penetration resistance, ensuring uniformity across all experimental units. Additionally, aggregates were collected for tensile strength and stability analyses.

2.4 Soil Analysis

2.4.1 Particle Size Distribution

The clay fraction was quantified using the pipette method, sand by sieving, and the silt fraction by considering the

Table 2 Characterization of the pyrolytic biochars used in the study

Attributes	Sewage sludge biochar added with cashew pruning residue	Cashew bagasse biochar
Granulometry (mesh)*		
1.0 to 2.0 mm (%)	52.50	31.46
1.0 to 0.5 mm (%)	21.50	38.38
0.5 to 0.25 mm (%)	13.75	19.12
0.25 to 0.105 mm (%)	8.37	8.54
0.105 to 0.053 (%)	2.24	1.95
< 0.053 mm (%)	1.64	0.55
BD (g cm^3)	0.28 ± 0.004	0.55 ± 0.004
EC (mS cm^{-1})	0.8 ± 0.100	2016.6 ± 28.67
pH	9.1 ± 0.100	9.61 ± 0.003
Moisture (%)	1.9 ± 0.200	1.74 ± 0.200
Volatile matter (%)	31.2 ± 0.700	43.27 ± 1.600
Ash content (%)	51.2 ± 1.900	22.65 ± 1.100
Fixed carbon (%)	15.6 ± 1.500	32.27 ± 1.140
C (g/kg)	348 ± 9.000	480.10 ± 34.00
N (g/kg)	24.45 ± 0.200	27.09 ± 0.060
P (g kg^{-1})	17.1 ± 2.500	11.62 ± 0.262
K (g kg^{-1})	6.1 ± 0.600	7.708 ± 0.271
Ca (g kg^{-1})	19.3 ± 2.800	1.948 ± 0.224
Mg (g kg^{-1})	7.3 ± 1.100	4.538 ± 0.177
Cu (g kg^{-1})	0.17 ± 0.020	0.051 ± 0.001
Fe (g kg^{-1})	15.3 ± 2.400	0.768 ± 0.141
Mn (g kg^{-1})	0.39 ± 0.030	0.045 ± 0.001
Mo (g kg^{-1})	0.01 ± 0.001	0.001 ± 0.0001
Zn (g kg^{-1})	1.39 ± 0.220	0.059 ± 0.015
Na (g kg^{-1})	4.09 ± 0.440	0.353 ± 0.027
Al (g kg^{-1})	26.8 ± 4.160	1.353 ± 0.252
Cd (g kg^{-1})	0.001 ± 0.001	ND
Pb (g kg^{-1})	0.016 ± 0.001	0.001 ± 0.00005
Cr (g kg^{-1})	0.040 ± 0.005	0.002 ± 0.0002
Ni (g kg^{-1})	0.023 ± 0.002	0.004 ± 0.00009
Ba (g kg^{-1})	0.221 ± 0.017	0.011 ± 0.001

ND Not determined, as the levels in the precursor sewage sludge were below the detection limit

*Standard deviation not calculated (n = 1). (±) Standard deviation (n = 3). For the quantification of nutrient levels in the biochars, the extracts were obtained as suggested in Enders and Lehmann (2012)—(Modified dry ash). After extraction, the P content was determined by the colorimetric method of the molybdovanadophosphoric acid (MAPA). The P content was estimated using a spectrophotometer at 400 nm. The levels of Ca, Mg, Cu, Fe, Mn, Mo, Zn, Al, Cd, Pb, and Cr were analyzed by ICP-OES, and K and Na by flame photometry. EC and pH were obtained according to the protocols described in Rajkovic et al. 2011. The determination of immediate analysis: moisture, volatile solids, ash, and fixed carbon followed the methodology described in ASTM D'1762–8. EC – Electrical conductivity, BD – Bulk density. The granulometry of the biochars was classified according to IBI (2015)

total mass of the soil sample used for analysis minus the sum of the sand and clay fractions. Sodium hydroxide (NaOH) 1 mol L^{-1} was used for the chemical dispersion of the particles (Gee and Bauder 1986).

2.4.2 Particle Density

It was determined using the volumetric flask method, utilizing oven-dried fine soil (105 °C) and ethyl alcohol,

where the principle is to determine the volume of alcohol used to fill a 50 mL volumetric flask containing 20 g of oven-dried fine soil (Blake and Hartge 1986a).

2.4.3 Bulk Density

It was measured using the volumetric ring method, calculating the ratio between the mass of soil dried at 105 °C and the volume of the ring (Blake and Hartge 1986b).

2.4.4 Total Porosity

Total porosity (α) was calculated using the soil bulk density (BD) and particle density (PD) data, using Eq. 1

$$\alpha = 1 - BD/PD \tag{1}$$

2.4.5 Soil Water Retention Curve

The water content at saturation (matric potential equal to 0 kPa) was considered equal to the total soil porosity (α, $m^3\ m^{-3}$); in addition to the saturation point, the soil water content was considered in equilibrium with the following matric potentials: −2, −4, −6, −8, −10, −33, −100, −700, and −1500 kPa. After obtaining the soil moisture values at all points, the data were fitted to the mathematical model proposed by van Genuchten (1980), Eq. 2,

$$\theta = \theta_r + \frac{\theta_s - \theta_r}{\left[1 + (\alpha|\phi_m|)^n\right]^m} \tag{2}$$

in which: θ is the water content ($m^3\ m^{-3}$); θ*r* and θ*s* are the residual and saturated water contents, respectively ($m^3\ m^{-3}$); ϕ*m* is the matric potential of soil water (kPa); α is the inverse of the air entry matric potential (kPa^{-1}); *m* and *n* are fitting parameters related to the shape of the curve. The data were fitted using the SWRC (Soil Water Retention Curve) program, following the Newton–Raphson iterative method, with *m* dependent on *n* (Dourado Neto et al. 2001).

This procedure was carried out at two points during the experiment: first, during the pre-incubation period, with biochar doses incorporated into the soil using unpreserved structure material; and second, at the end of the experiment, after 90 days (30 of incubation and 60 of cultivation), when samples were collected in volumetric rings, thus maintaining the preserved structure.

2.4.6 Soil Penetration Resistance

It was determined using preserved structure samples with moisture equilibrated at a matric potential of −33 kPa. An electronic static laboratory penetrometer equipped with a linear actuator system was used. It operated at a speed of 1 cm min^{-1}, featured a 20 kgf load cell, and included a rod with a cone having a base diameter of 0.4 cm, a 60° angle, and an area of 12.566 mm^2. This equipment records one reading per second. The penetrometer is connected to a computer for data collection via the equipment's software (Tormena et al. 1998). The procedure involves obtaining an average value representing the penetration resistance for each soil sample analyzed.

2.4.7 Tensile Strength of Aggregates

To analyze the tensile strength (TS) of aggregates, equipment with a linear electronic actuator at a constant speed of 0.03 mm s^{-1} was used (Tormena et al. 2008). Aggregates with a diameter between 19 and 25 mm were used; subsequently, the clods were weighed on an electronic balance. After this step, the clod was positioned as stably as possible between the two metal plates (lower and upper) of the equipment, which has a 20 kgf load capacity. The load value used to break the aggregate was recorded through an electronic data acquisition system. A portion of this aggregate was then collected and dried at 105ºC to determine the sample's residual moisture content.

Tensile strength was estimated according to Dexter and Kroesbergen (1985), using Eq. 3,

$$TS = \frac{(0{,}576P)}{D^2 10^3} \tag{3}$$

in which *TS* is the tensile strength of the clod (kPa), *0.576* is the proportionality constant relating the applied compressive stress to the tensile stress generated within the clod, *P* is the applied force (N), and *D* is the effective diameter of the clod (m); 10^3 is the conversion factor from Pa to kPa.

The effective diameter of the clod was measured using Eq. 4 (Watts and Dexter 1998),

$$D = Dm\left(\frac{M}{M_0}\right)^{0.333} \tag{4}$$

where D_m is the average diameter of the clods [(25 + 19)/2, em mm], explained by the average size of the sieve openings, *M* is the mass of the individual clod dried at (g), and M_o is the average mass of the clods dried at 105 °C (g).

2.4.8 Aggregate Stability

It was determined using the wet sieving method to measure the quantity and size distribution of water-stable aggregates compared to those that disintegrated during the sieving process (Kemper and Rosenau 1986). The equipment used for sieving was a vertical electric oscillator,

which holds two sets of sieves with mesh openings of 4.76, 2.0, 1.0, 0.5, and 0.25 mm. The mass of aggregates retained in each sieve was expressed in five diameter classes (7.93–4.76 mm, 4.76–2.00 mm, 2.00–1.00 mm, 1.00–0.50 mm, and 0.50–0.25 mm), allowing the estimation of the percentage of stable aggregates in each class according to Eq. 5,

$$\%SA = \left(\frac{Ma - Mp}{Ms - Mw - \sum Mp} \right) \times 100 \quad (5)$$

where *%SA* is the percentage of stable aggregates per class; *Ma* is the mass of apparent aggregates in the class, *Mp* is the mass of primary particles in the class, *Ms* is the mass of aggregates in the initial sample (25 g), and *Mw* is the mass of water in the initial sample.

The mean weight diameter (MWD), considered an index of soil aggregation (van Bavel 1950), was calculated by summing the products of the mean diameter (*Xi*) and the fraction (*Wi*) of stable aggregates in each class, Eq. 6,

$$\text{MWD} = \sum (Xi.Wi) \quad (6)$$

2.5 Plant Analysis

At the end of the experiment, when the plants reached the pollination stage, R1 – silking, characterized by the presence of visible stigmas, the following parameters were evaluated: culm height and plant height, measured with a tape from the soil surface to the top of the last culm and the apex of the last emitted leaf, respectively; culm diameter, measured with a digital caliper, using the average value from three measurements. The plants and roots were collected separately, placed in paper bags, and dried in an oven at 65 °C until a constant mass was achieved to determine the dry biomass.

2.6 Data Analysis

The normality of the residuals was verified using the Shapiro–Wilk test, and the homogeneity of variances was assessed with Bartlett's test. When necessary, data transformation was performed using the Box and Cox (1964) procedure to find an optimal power (λ) such that the transformed data would approximate a normal distribution.

Initially, analysis of variance was conducted using the F-test; mean comparisons were made using Dunnett's test (where each treatment was compared exclusively with the control) and Tukey's test (all treatments were compared among themselves), both at a 5% significance level. The data were analyzed considering a completely randomized design, in a 2 × 4 factorial arrangement (two biochars: sewage sludge added to cashew pruning in a 1:1 ratio, and cashew bagasse, produced by pyrolysis; four doses: 5, 10, 20, and 40 Mg ha^{-1}) plus the control, with four repetitions. For the water retention curve data, a completely randomized design in a 2 × 2 × 4 factorial arrangement was considered (two biochars: sewage sludge added to cashew pruning in a 1:1 ratio, and cashew bagasse, produced by pyrolysis; two periods: pre-incubation and post-cultivation; four doses: 5, 10, 20, and 40 Mg ha^{-1}) plus the control, with four repetitions.

To determine the best-fit curve, linear, quadratic, and cubic polynomial models were tested, with model selection based on the coefficient of determination (R^2) and the statistical significance of the regression parameters ($p < 0.05$ and 0.01). In cases where the data exhibited non-linear behavior that simpler models could not adequately describe, the cubic model was employed to enhance predictive accuracy. Furthermore, the experimental design – comprising five dose levels replicated five times – provided sufficient statistical robustness to justify using more complex models without risking overfitting. All analyses were conducted using SAS® OnDemand for Academics.

3 Results and Discussion

Biochar application significantly affected water depth (WD) and available water capacity (AWC) during incubation (WD-I and AWC-I), and cultivation (WD-C and AWC-C), as well as aggregate tensile strength (TS), the only attribute altered by at least one biochar dose. Significant interactions between biochar type and dose were observed for TS, AWC-I, and AWC-C (Table S1).

Dunnett's test (5% probability) identified significant differences for WD-I, TS, and AWC-I compared to the control, while other parameters (WD-C, BD, PR, MWD, and AWC-C) showed no differences (Table S2). Notably, cashew bagasse biochar (CBB) at 5 and 40 Mg ha^{-1} reduced WD-I by 49.8% and 32.2%, respectively, suggesting lower doses for optimizing water use efficiency.

For TS (S2), significant reductions were observed with sewage sludge biochar combined with cashew pruning at 20 and 40 Mg ha^{-1} (SSPB20, SSPB40) and cashew bagasse at 40 Mg ha^{-1} (CBB40), with TS values indicating slightly hard to soft consistency (Oliveira et al. 2020). However, SSPB10 increased TS to 66.89 kPa, corresponding to a very hard consistency.

Regarding AWC-I (Table S2), significant effects were found for SSPB at 5, 10, and 20 Mg ha^{-1}, which reduced AWC by 21% on average, while all CBB treatments

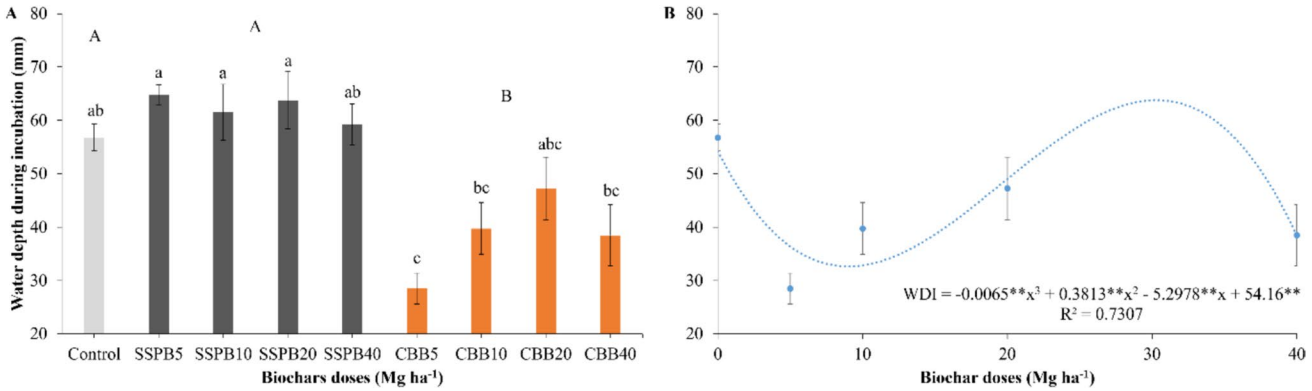

Fig. 2 Mean values of water depth required during the incubation period for control treatments and sewage sludge biochar added with cashew pruning residue (SSPB) and cashew bagasse biochar (CBB) to maintain the soil between field capacity and consumption up to 30% of available water capacity (**A**). Regression between water depths required during the incubation period and doses of CBB (**B**). Means followed by the same lowercase letter are not significantly different by Tukey's test at a 5% significance level; uppercase letters compare treatment groups (control, SSPB, CBB), with the same uppercase letter indicating no significant difference by Tukey's test at a 5% significance level. Bars represent the standard error of the mean. **Significant at the 1% probability level

increased AWC by 27%. No significant differences were observed for WD-C, BD, PR, MWD, or AWC-C.

3.1 Water Depth in the Incubation Period (WD-I)

The highest water consumption during the incubation period was observed in SSPB5, SSPB10, and SSPB20, with mean values of 64.75 mm, 61.50 mm, and 63.75 mm, respectively (Fig. 2A). In contrast, SSPB40 and the control showed lower means (59.25 mm and 56.75 mm).

Cashew bagasse biochar treatments exhibited the lowest water use, with CBB5 requiring only 28.50 mm, not differing significantly from CBB10, CBB20, and CBB40 (39.75 mm, 47.30 mm, and 38.50 mm, respectively). Among them, CBB20 was the only treatment that did not statistically differ from others.

Tukey's test indicated that treatments with cashew bagasse biochar consumed significantly less water (38.50 mm on average) compared to the control and sewage sludge biochar treatments (56.75 mm and 62.31 mm, respectively), which did not differ from each other but had higher water consumption than CBB treatments.

A significant cubic correlation was observed for cashew bagasse biochar treatments (Fig. 2B), identifying optimal doses for water retention. For agronomic purposes, the model predicts that 9 Mg ha^{-1} minimizes water consumption (32.63 mm), reducing water requirements by approximately 40% compared to untreated soil.

Several factors explain the findings of this study. The granulometry of SSPB indicates that more than half of its particles range between 1.0 and 2.0 mm (Table 2), which reduces its specific surface area – concerning CBB – and limits water adsorption. The interaction of biochar with water also depends on its hydrophilic or hydrophobic properties, which are influenced by functional groups and feedstock composition (Eibisch et al. 2015). CBB is hydrophilic and contains oxygen-rich functional groups (hydroxyl, carbonyl, and carboxyl) that facilitate hydrogen bonding, thereby enhancing water retention (Fregolente et al. 2023).

Biochar properties can change over time due to soil aging, involving chemical reactions, physical processes, and microbial activity, which increase surface charges and interactions with soil components (Zornoza et al. 2016). Additionally, biochar incorporation into sandy soils can alter soil structure by filling voids between mineral grains, reducing bulk density and increasing total porosity (Zanutel et al. 2024). This structural modification explains the higher water retention observed at elevated CBB doses, as smaller pores (micropores) within aggregates increase the water layer required to maintain field capacity.

3.2 Water Depth in the Cultivation Period (WD-C)

During the cultivation period, the irrigation layer did not significantly differ between treatments, suggesting changes in biochar-soil–water interactions in the presence of plants compared to the incubation period (Fig. 3). Plant water uptake increased the required water layer to maintain soil moisture between field capacity and the irrigation threshold. In uncultivated soils, water loss primarily occurs through surface evaporation, while in cultivated soils, transpiration becomes dominant. Root absorption from subsurface layers and subsequent transpiration often surpass direct soil evaporation rates (Weil and Brady 2016).

During early corn growth stages, evaporation dominates evapotranspiration, but as the crop develops, transpiration

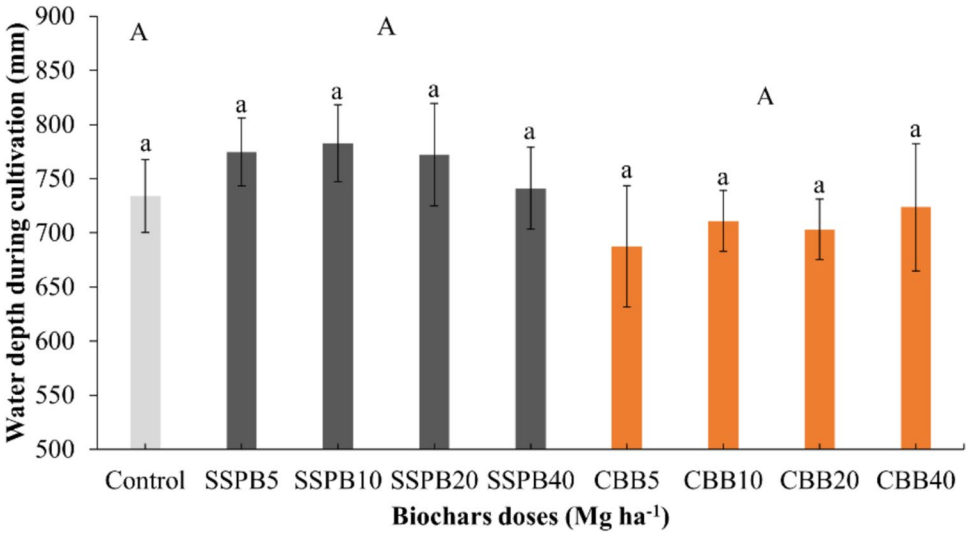

Fig. 3 Mean values of water depth required during the incubation period for control treatments and sewage sludge biochar added with cashew pruning residue (SSPB) and cashew bagasse biochar (CBB) to maintain the soil between field capacity and consumption up to 30% of available water capacity. Means followed by the same lowercase letter are not significantly different by Tukey's test at a 5% significance level; uppercase letters compare treatment groups (control, SSPB, CBB), with the same uppercase letter indicating no significant difference by Tukey's test at a 5% significance level. Bars represent the standard error of the mean

becomes the primary component. Kimball et al. (2019) reported that evaporation accounts for 70% of evapotranspiration until the V6 stage, whereas transpiration dominates thereafter, removing more water from the soil.

Biochar incorporation is known to enhance soil aggregation and soil structure, which, in turn, can improve water retention and reduce the need for irrigation (Zhang et al. 2020). However, in our 90-day experiment, the biochar effects were insufficient to reduce water consumption in the treated soils compared to the control. This result could be attributed to the balance between biochar's potential to increase water retention and the possible enhancement of evapotranspiration through plant growth. Increased root water uptake, along with the creation of preferential flow paths in the soil, may lead to a non-uniform distribution of water, potentially offsetting the benefits of biochar in water retention. In addition, no drainage losses were observed at the column bases, suggesting that the water applied remained within the treated layers, which may explain the absence of significant differences in water application during the cultivation period.

In line with Blanco-Canqui (2017), biochar's influence on water dynamics extends beyond retention to include the infiltration and hydraulic conductivity of water within soils. For example, biochar has been shown to alter both saturated and unsaturated hydraulic conductivity, with effects varying based on soil texture. In coarse-textured soils, biochar often reduces hydraulic conductivity due to the clogging of soil macropores by fine particles, which can limit water infiltration. On the other hand, biochar can improve water flow in fine-textured soils, such as clay loams, by enhancing soil aggregation and increasing macroporosity. This is particularly relevant in the context of improving water flow in compacted soils or soils with low infiltration rates, which can increase water capture and storage, reducing runoff and nutrient leaching.

Moreover, the impact of biochar on plant-available water is often linked to the increased porosity and specific surface area of its particles, which allows for greater retention of water (Edeh et al. 2020). Thus, while biochar holds promise as a tool to enhance soil water retention and reduce irrigation needs, the dynamics of its effects are complex and require further exploration to better understand its interactions with soil, water, and plant growth.

3.3 Bulk Density (BD)

BD did not differ significantly between treatments (Fig. 4A). However, SSPB doses showed a significant correlation, fitting a quadratic model that estimated a BD reduction to 1.49 g cm^3 at 22.6 Mg ha^{-1} (Fig. 4B). Compared to the initial BD of 1.55 g cm^3, this represents an approximate 4% decrease.

SSPB has a lower density (0.28 g cm^3) than CBB (0.55 g cm^3) (Table 2) and a larger particle size. Consequently, SSPB is expected to reduce soil bulk density more effectively, as its lower density increases the total volume added to the soil (Lim et al. 2016). This aligns with studies showing that biochar incorporation decreases bulk density due to its lower density compared to mineral soil particles

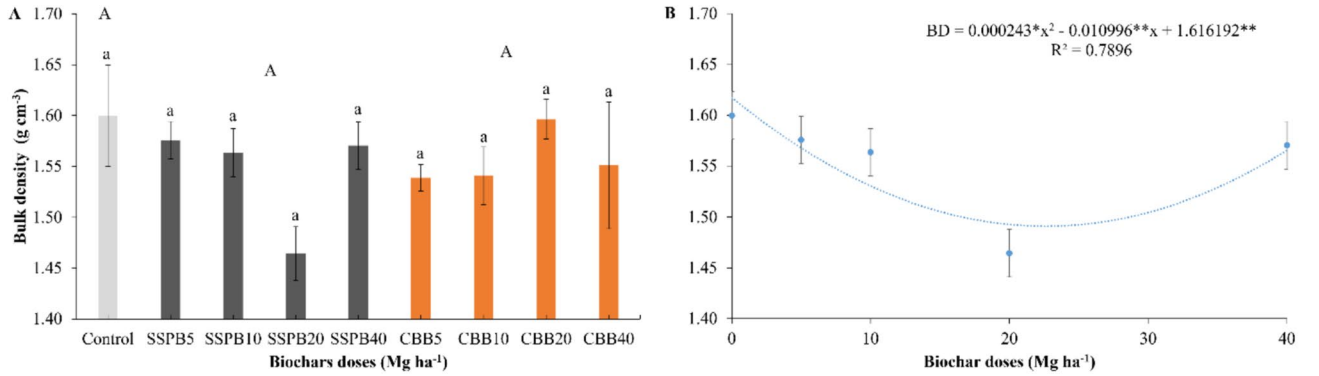

Fig. 4 Mean values of soil resistance to penetration for control treatments and sewage sludge biochar added with cashew pruning residue (SSPB) and cashew bagasse biochar (CBB) at a matric potential of −33 kPa (**A**). Regression between soil resistance to penetration and doses of SSPB (**B**). Means followed by the same lowercase letter are not significantly different by Tukey's test at a 5% significance level; uppercase letters compare treatment groups (control, SSPB, CBB), with the same uppercase letter indicating no significant difference by Tukey's test at a 5% significance level. Bars represent the standard error of the mean. **Significant at the 1% probability level

(Blanco-Canqui 2017), enhancing porosity, aggregation, and soil structure (Verheijen et al. 2019).

The reduction in BD by SSPB can influence key soil physical properties, including total porosity, mechanical resistance to root penetration, and water retention. In a study using cashew bagasse biochar in a cohesive Typic Haplustult, BD significantly decreased with increasing biochar doses, reaching a maximum reduction at 40 Mg ha^{-1} (Nascimento et al. 2024). In the present study, using the same biochar but in a Planosol with loamy-sandy texture, the maximum BD reduction occurred at 22.6 Mg ha^{-1}.

Biochar-induced BD reduction is generally more pronounced in clayey soils than in sandy ones, as biochar promotes pore formation and aeration in finer-textured soils (Bekchanova et al. 2024). However, in sandy soils, BD reduction depends on biochar particle size (Chen et al. 2018). Biochar with larger particles (88% greater than 1 mm) applied to sandy and loamy-clay soils at 24 and 120 Mg ha^{-1} reduced BD by 4%–20% and 18%–26%, respectively (Lim et al. 2016). Consistent with these findings, the present study observed BD reduction with SSPB addition, which had a larger particle fraction (52.50% greater than 1 mm) compared to CBB (31.46% greater than 1 mm) (Fig. 4B).

3.4 Penetration Resistance (PR)

No statistical differences in PR were observed between doses or between the control and biochars (Fig. 5A). However, a significant correlation was found for SSPB, with a cubic polynomial fit, identifying doses where PR reaches its maximum and minimum (Fig. 5B). The soil, degraded

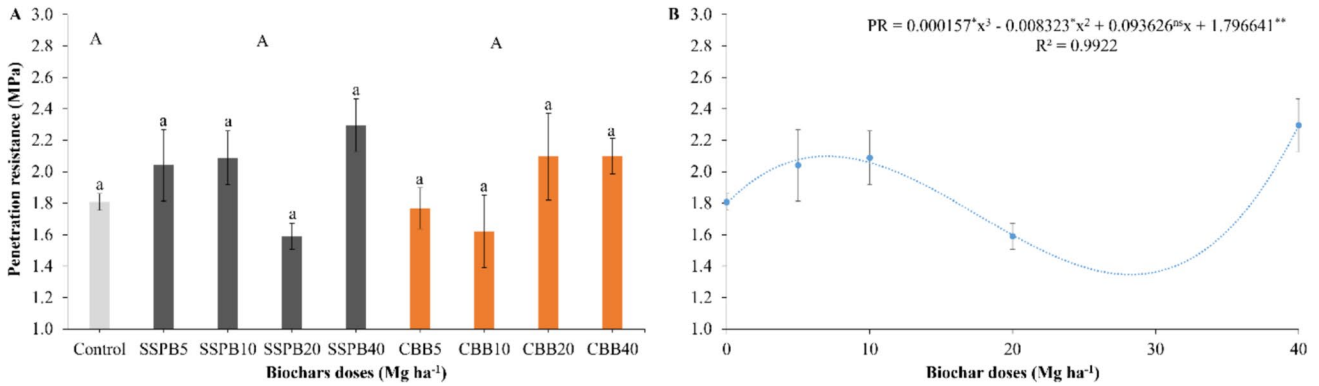

Fig. 5 Mean values of soil resistance to penetration for control treatments and sewage sludge biochar added with cashew pruning residue (SSPB) and cashew bagasse biochar (CBB) at a matric potential of −33 kPa (**A**). Regression between soil resistance to penetration and doses of SSPB (B). Means followed by the same lowercase letter are not significantly different by Tukey's test at a 5% significance level; uppercase letters compare treatment groups (control, SSPB, CBB), with the same uppercase letter indicating no significant difference by Tukey's test at a 5% significance level. Bars represent the standard error of the mean. **Significant at the 1% probability level

by overgrazing and compaction, benefited from biochar application. The model predicts that a dose of 28.3 Mg ha^{-1} of SSPB reduces PR to 1.34 MPa, a 36.2% decrease compared to the control. This reduction is crucial, as it lowers soil mechanical resistance to levels that do not restrict root growth. In the control treatment, PR averaged 1.8 MPa, close to the critical threshold of 2 MPa for root development (Silva et al. 1994; Tormena et al. 1998).

In addition, our findings align with Nascimento et al. (2024), who observed significant reductions in soil penetration resistance (− 16.2 and − 16.1%) when biochar was applied at doses of 20 and 40 Mg ha − 1, which was associated with improvements in soil porosity and the promotion of silicon adsorption.

The PR result aligns with the reduction in BD, attributed to biochar granulometry, which decreases contact points between soil mineral particles, leading to lower BD and reduced PR and aggregate tensile strength (TS) (Zong et al. 2014). Most studies report no significant PR effects after biochar addition, but Busscher et al. (2010) found a decrease in PR with a 44 Mg ha^{-1} dose of biochar produced from pecan *(Carya illinoinensis)* shells, suggesting that higher biochar doses are needed to notably reduce PR. Additionally, biochar may require long periods to interact with soil particles before significantly reducing compaction.

The larger SSPB particles create a structure with larger pores and fewer contact points with soil particles, lowering cohesion and making the soil matrix less resistant to root penetration. SSPB also contains higher levels of cations (Ca^{2+}, Mg^{2+}, K^{+}, Zn^{2+}, Ni^{2+}, Fe^{2+}, Fe^{3+}, Cu^{2+}, Mn^{2+}) that promote particle flocculation, reducing BD, PR, and improving aggregate stability (Li et al. 2023). However, SSPB's higher Na^{+} levels (Table 2) can cause negative effects, such as clay dispersion, reducing porosity and increasing BD, which may explain the increase in PR at higher doses (> 30 Mg ha^{-1}) (Haghnia and Pratt 1988; Stavi et al. 2021).

3.5 Tensile Strength of Aggregates (TS)

Statistical differences were observed in the TS between doses and between the control and biochars (Fig. 6A). SSPB10 exhibited the highest TS (66.89 kPa), followed by CBB10, control, SSPB5, CBB20, and CBB40, which did not differ significantly (averages of 34.28, 33.76, 32.81, 30.23, and 22.93 kPa, respectively). CBB5 had the lowest TS at 21.31 kPa, while SSPB20 had the lowest average at 17.97 kPa. SSPB and control showed higher TS values compared to CBB (Fig. 6A).

The 10 Mg ha^{-1} dose of SSPB resulted in higher TS than the 20 Mg ha^{-1} dose, indicating an initial increase followed by a reduction. This pattern may be attributed to the effects of biochar on soil aggregation and porosity. At lower doses, biochar may promote improved soil aggregation, enhancing the soil's structural integrity and increasing TS. However, at higher doses, biochar can introduce changes in soil porosity and water retention, which may lead to reduced compaction and a subsequent decrease in TS. These changes in TS reflect alterations in soil cohesion, which are important for plant growth, as they influence root penetration and water movement (Nascimento et al. 2024).

In the SSPB regression (Fig. 6B), the 7.91 Mg ha^{-1} dose led to a maximum TS of 53.1 kPa, classifying the dry aggregates as hard (Oliveira et al. 2020). However, the cubic model's parameters suggested a negative TS value at the function's minimum, a mathematically derived estimate, which

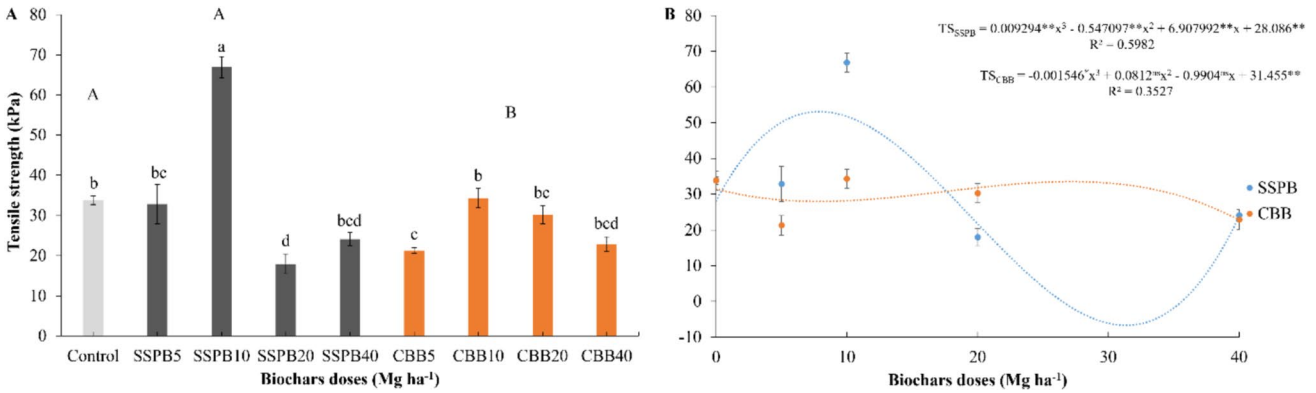

Fig. 6 Mean values of aggregate tensile strength (TS) for control treatments and sewage sludge biochar added with cashew pruning residue (SSPB) and cashew bagasse biochar CBB) (**A**). Regression between tensile strength and doses of SSPB and CBB (**B**). Means followed by the same lowercase letter are not significantly different by Tukey's test at a 5% significance level; uppercase letters compare treatment groups (control, SSPB, CBB), with the same uppercase letter indicating no significant difference by Tukey's test at a 5% significance level. Bars represent the standard error of the mean. ^{ns} not significant; ** and * Significant at the 1% and 5% probability level, respectively

is not physically feasible, like situations in van Genuchten (1980) model estimations (Yang and You 2013).

In agricultural soils, the incorporation of biochar from sewage sludge and cashew pruning is recommended, as it alters the consistency of soil aggregates. The addition of biochar increases the TS from slightly hard (28.09 kPa) in the control to hard (53.1 kPa) at a dose of 7.91 Mg ha^{-1}, which improves resistance to mechanical dispersion during soil preparation (Reis et al. 2014). However, TS values below 65 kPa (Oliveira et al. 2020) do not indicate overly cohesive aggregates, and the aggregates remain friable in moist conditions, allowing for root growth.

In contrast, the TS of aggregates with cashew bagasse biochar (CBB) ranged between 27.94 and 33.49 kPa, indicating slightly hard consistency at doses of 7.86 and 27.16 Mg ha^{-1}. Given the minimal changes in TS, CBB application is not recommended solely for modifying aggregate TS due to the low cost/benefit ratio.

High TS values are associated with greater resistance to rupture, which is beneficial for soil stability, but excessive cohesion can hinder crop growth, particularly in compacted soils with high clay content. Biochars, like SSPB, increase TS at lower doses by enhancing particle cohesion and stabilizing aggregates. However, at higher doses, biochar improves porosity and reduces tensile resistance (Goldan et al. 2022). Biochar generally reduces TS by 42% to 242%, as reported by Blanco-Canqui (2017), highlighting its potential to alter soil structure.

3.6 Weight Mean Diameter of Soil Aggregates (WMD)

Significant differences in the WMD were observed between doses but not between the control and the biochars (Fig. 7). SSPB10 resulted in the highest WMD (5.97 mm), while CBB10 had the lowest (4.40 mm). The control, SSPB5, SSPB20, SSPB40, CBB5, CBB20, and CBB40 treatments did not differ significantly, with average values ranging from 4.47 to 5.80 mm.

The significant increase in the WMD, particularly observed in the SSPB10 treatment (10 Mg ha^{-1} of sewage sludge and cashew pruning biochar), indicates improved soil aggregate stability. This parameter reflects the size distribution of water-stable aggregates, with higher values indicating a greater proportion of macroaggregates relative to microaggregates (Kemper and Rosenau 1986; Rui et al. 2022). The formation of these stable macroaggregates has important implications for soil physical quality, enhancing water infiltration, aeration, and resistance to erosion while maintaining adequate water retention capacity (Six et al. 2000).

The enhanced aggregation observed at the 10 Mg ha^{-1} SSPB dose can be attributed to two primary mechanisms. First, the biochar's rich content of flocculating cations (Ca^{2+}, Mg^{2+}, Zn^{2+}, Ni^{2+}, Fe^{2+}, Fe^{3+}, Cu^{2+}, and Mn^{2+}) promoted particle association through electrostatic interactions, neutralizing negative charges on clay particles and biochar surfaces (Li et al. 2023). Second, the nutrient-rich composition of SSPB likely stimulated microbial activity, leading to increased production of organic binding agents that cement soil particles, as previously demonstrated by Junior and Guo (2023) in similar biochar-amended systems.

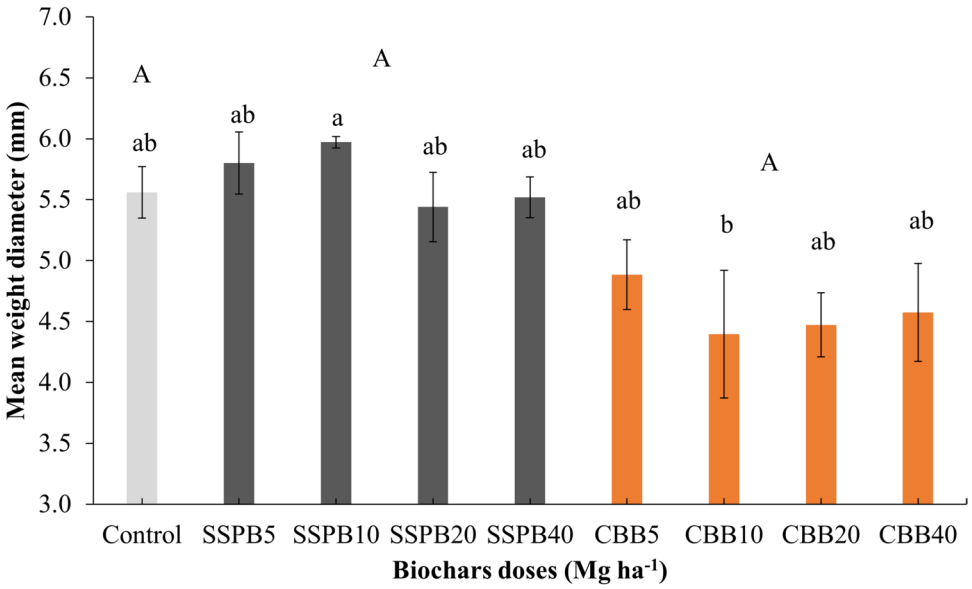

Fig. 7 Mean values of mean weight diameter (MWD) for control treatments and sewage sludge biochar added with cashew pruning residue (SSPB) and cashew bagasse biochar (CBB). Means followed by the same lowercase letter are not significantly different by Tukey's test at a 5% significance level; uppercase letters compare treatment groups (control, SSPB, CBB), with the same uppercase letter indicating no significant difference by Tukey's test at a 5% significance level. Bars represent the standard error of the mean

Notably, all treatments maintained WMD values above 0.5 mm, the established threshold for erosion-resistant aggregates (Kiehl 1979), which was particularly remarkable given the sandy texture of the experimental soil. This unexpected result highlights the significant role of maize rhizosphere effects, where root exudates and associated microbial activity contributed to aggregate stabilization across all treatments (Bronick and Lal 2005). However, the absence of significant differences in root biomass among treatments suggests that biochar amendments and rhizosphere processes acted synergistically rather than independently to enhance aggregate stability.

These findings underscore the potential of SSPB as a soil amendment for improving structural quality in sandy soils, with the 10 Mg ha^{-1} dose showing promise. However, the study also reveals an important methodological consideration: under field conditions with active plant growth, it becomes challenging to isolate the specific effects of biochar from natural rhizosphere processes. This complexity suggests the need for complementary controlled experiments to better understand the individual and combined mechanisms governing aggregate stabilization in biochar-amended soils.

3.7 Soil Water Retention Curve (SWRC)

Significant statistical differences were observed for the van Genuchten (1980) equation parameters and available water capacity (AWC) at a 1% significance level, indicating effects of doses, periods, and interaction on soil water retention curves (Table S3). Significant differences were found between periods (pre-incubation and post-cultivation) and between biochars (Table 3). A SWRC (Fig. 8) can only be considered identical to another if there are no significant differences in the van Genuchten parameters (Jorge et al. 2010); thus, all treatments exhibited distinct curves.

The saturated water content (θs), representing total porosity, was consistently higher during the pre-incubation period for both biochars, with observed reductions attributed to particle rearrangement over the 90-day experimental duration. In the pre-incubation phase, CBB5 exhibited the highest θs value (0.426 cm^3 cm^{-3}), showing a 6.5% increase over the control, while SSPB10 showed the lowest (0.387 cm^3 cm^{-3}), though these differences were not statistically significant.

Post-cultivation, notable θs increases were observed for CBB5 (7.4%), CBB40 (9.1%), and SSPB20 (9.4%) compared to the control, demonstrating the beneficial effects of biochar on soil structure through enhanced aggregation, increased porosity, and reduced bulk density (Blanco-Canqui 2017). These findings align with Chen et al. (2018), who reported a 51.4% porosity increase in sandy soils amended with wheat straw biochar (150 Mg ha^{-1}) due to improved macroporosity and reduced compaction.

Table 3 Mean values of the parameters of the soil water retention curve according to the van Genuchten (1980) model as a function of biochar doses applied to the soil during the pre-incubation (PI) and post-cultivation (PC) periods

Doses	α-PI	α-PC	m-PI	m-PC	n-PI	n-PC	θr-PI	θr-PC	θs-PI	θs-PC	AWC-PI	AWC-PC
Mg ha^{-1}	—kPa^{-1}—						——————cm^3 cm^{-3}——————					
Control												
0	0.476 Aa	0.258 Bbc	0.414 Acd	0.269 Ba	1.709 Ac	1.369 Ba	0.038 Abc	0.009 Ba	0.400 Aab	0.350 Bab	0.118 Bc	0.189 Aab
Sewage sludge biochar added with cashew pruning residue												
5	0.598 Aa	0.186 Bbc	0.427 Abcd	0.287 Ba	1.750 Abc	1.402 Ba	0.047 Aab	0.011 Ba	0.414 Aab	0.350 Bab	0.088 Bd	0.240 Aa
10	0.383 Aa	0.132 Bc	0.541 Aa	0.302 Ba	2.044 Aa	1.434 Ba	0.054 Aa	0.008 Ba	0.387 Ab	0.332 Bb	0.090 Bd	0.213 Aa
20	0.365 Aa	0.387 Aabc	0.488 Aabc	0.276 Ba	1.967 Aab	1.416 Ba	0.052 Aa	0.008 Ba	0.403 Aab	0.383 Ba	0.100 Bcd	0.180 Aabc
40	0.334 Aa	0.281 Aabc	0.498 Aab	0.291 Ba	2.000 Aa	1.410 Ba	0.053 Aa	0.010 Ba	0.411 Aab	0.360 Bab	0.103 Bcd	0.190 Aabc
Cashew bagasse biochar												
5	0.598 Aa	0.306 Aa	0.350 Ade	0.306 Aa	1.540 Acd	1.445 Aa	0.037 Ac	0.014 Ba	0.426 Aa	0.376 Ba	0.168 Aa	0.162 Ac
10	0.383 Aa	0.259 Ba	0.327 Ae	0.259 Ba	1.466 Ad	1.350 Aa	0.034 Ac	0.009 Ba	0.416 Aab	0.356 Bab	0.161 Ab	0.156 Ac
20	0.365 Aa	0.263 Ba	0.372 Ade	0.263 Ba	1.625 Acd	1.358 Ba	0.051 Aa	0.011 Ba	0.419 Aab	0.351 Bab	0.143 Bb	0.168 Abc
40	0.334 Aa	0.298 Ba	0.397 Ade	0.298 Ba	1.668 Acd	1.430 Ba	0.054 Aa	0.009 Ba	0.414 Aab	0.382 Ba	0.142 Bb	0.203 Aab

For the comparison of the same variable, means followed by the same uppercase letter in the row do not differ by Tukey's test at a 5% significance level. For the same variable, means followed by the same lowercase letter in the column do not differ by Tukey's test at a 5% significance level

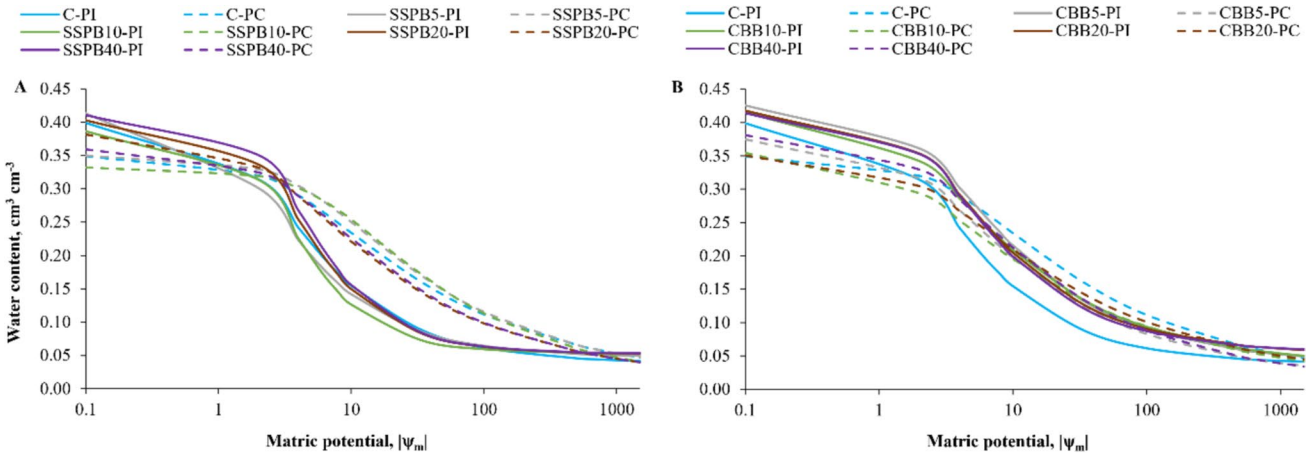

Fig. 8 Water retention curves for soil for control treatments and sewage sludge biochar added with cashew pruning residue (SSPB) (**A**) and cashew bagasse (CBB) (**B**) during pre-incubation (PI) and post-cultivation (PC) periods. C – Control; SSPB5, SSPB10, SSPB20, and SSPB40 – Sewage sludge biochar added with cashew tree pruning at doses of 5, 10, 20 and 40 Mg ha^{-1}, respectively; CBB5, CBB10, CBB20, and CBB40 – Cashew bagasse biochar at doses of 5, 10, 20 and 40 Mg ha^{-1}, respectively

Significant variations in the van Genuchten parameters α, m, and n (curve shape parameters) between periods and biochar types (van Lier and Pinheiro 2018; Nascimento et al. 2018a) confirmed distinct SWRC shapes, reflecting pore-size distribution changes sensitive to structural modifications (Nascimento et al. 2018b). Figure 8 illustrates that higher biochar doses increased soil moisture from saturation to Ψm = −6 kPa (macroporosity range), confirming macroporosity gains and consequent total porosity enhancement, particularly during cultivation as biochar-soil interactions intensified.

The residual water content (θr), analogous to the permanent wilting point (PWP), decreased post-incubation, indicating improved soil water release efficiency (Zusevics 1980). This aligns with Wei et al. (2023), who documented a 4.2% PWP reduction in medium-textured soils after biochar application, correlating with porosity increases. Plant-available water (AWC-PI) significantly increased post-cultivation for most treatments, except at 5–10 Mg ha^{-1} doses, enhancing soil water retention and availability (Garg et al. 2019; Sun et al. 2013; Verheijen et al. 2019). CBB outperformed SSPB in AWC during pre-incubation, with CBB5 showing the highest AWC (0.168 cm^3 cm^{-3}), attributed to its hydrophilic nature (Fregolente et al. 2023).

Notably, CBB5 also demonstrated optimal water-use efficiency, combining technical feasibility with improved hydraulic properties.

Table 4 Mean values for the growth attributes of maize (*Zea mays* L.) plants: culm diameter (CD), culm height (CH), plant height (PH), shoot dry mass (SDM), root dry mass (RDM), and total dry mass (TDM)

Treatments	CD	CH	PH	SDM	RDM	TDM
	mm	cm		g plant^{-1}		
Control	18.30	218.25	238.50	520.00	2.29	175.63
SSPB5	20.44	211.75	228.75	545.00	2.32	197.10
SSPB10	19.76	209.75	224.25	524.50	2.25	187.11
SSPB20	22.32*	198.75	211.25	509.25	2.39	204.35
SSPB40	20.01	177.75	187.00*	532.50	2.23	169.19
CBB5	21.18	197.50	206.75	537.50	2.22	171.85
CBB10	19.62	198.25	214.50	502.50	2.25	189.69
CBB20	21.12	194.00	212.75	531.25	2.20	178.80
CBB40	20.58	203.00	229.25	450.25	2.29	169.22

Biochars from the co-pyrolysis of sewage sludge and cashew pruning biomass (SSPB) and cashew bagasse (CBB) at doses of 5, 10, 20, and 40 Mg ha^{-1}, respectively; CBB5, CBB10, CBB20, and CBB40 biochars from cashew bagasse at doses of 5, 10, 20, and 40 Mg ha^{-1}, respectively

*Represents the significant difference of the treatment mean compared to the control treatment mean by Dunnett's test at 5% significance

These results underscore biochar's potential to modulate soil–water dynamics, with dose- and type-dependent effects on porosity, water retention, and plant-available water.

3.8 Plant Growth

Regarding maize plant attributes (S4), variance analysis did not detect significant effects of any variation sources on culm height (CH), culm diameter (CD), shoot dry mass (SDM), root dry mass (RDM), or total dry mass (TDM) at 1% and 5% probability levels. However, significant interaction effects were observed for plant height (PH) at the 5% probability level (Table 4).

Statistical analysis using Dunnett's test ($\alpha = 0.05$) revealed no significant differences between biochar treatments and the control for culm height, shoot dry mass, root dry mass, or total dry mass (Table 4). However, a notable exception was observed in CD, where the SSPB20 treatment (20 Mg ha^{-1} sewage sludge and cashew pruning biochar) showed a 22% increase (22.32 mm vs. 18.30 mm in control), enhancing plant structural robustness against environmental stresses (Losey et al. 2002; Stubbs et al. 2020). Conversely, SSPB40 treatment reduced plant height by 22% (187 cm vs. control), representing a 12% reduction from the expected height (213 cm) for the BRS2022 hybrid (Pacheco et al. 2009). These morphological changes occurred without significant biomass alterations, suggesting a phenotypic shift toward more compact plants.

There was no significant differences in PH, CD, or biomass parameters across treatments. This uniformity likely resulted from standardized mineral fertilization, which may have overshadowed potential biochar effects (Scotti et al. 2022). Nevertheless, pooled biochar treatments (CBB and SSPB) significantly increased CD compared to the control, with SSPB20 showing the maximum effect (22.32 mm). These findings align with Tanure et al. (2019), who reported 36.4% CD increase in maize with eucalyptus biochar, demonstrating biochar's synergistic effects on soil structure and plant growth.

The CD enhancement in SSPB20 correlated with improved soil physical properties: reduced bulk density, increased porosity, lower penetration resistance, and enhanced aggregate stability (MWD). These modifications created favorable conditions for cell expansion by improving water absorption (via increased turgor pressure) and nutrient availability (Ali et al. 2023; Shah et al. 2017). As Wang et al. (2022) demonstrated, soil compaction negatively impacts maize growth, highlighting the importance of structural improvements from biochar.

Notably, while SSPB20 improved CD, root biomass remained statistically unchanged across all treatments, indicating that biochar amendments did not negatively affect below-ground growth. Plant height, though genetically controlled (Chen et al. 2024), showed dose-dependent responses: CH and PH decreased linearly with increasing SSPB doses, while CD followed a quadratic trend, peaking at 21.9 mm with 23.2 Mg ha^{-1} SSPB (Fig. 9).

These responses suggest that biochar's primary influence occurred through soil physical modification rather than direct nutritional effects, particularly when mineral nutrition was optimized. The results underscore biochar's potential to enhance crop architecture and stress resistance while maintaining yield potential in well-fertilized systems.

While the study did not specifically aim to reduce plant height, the application of sewage sludge and cashew pruning biochar (SSPB) resulted in shorter plants without compromising dry biomass production. This morphological modification offers distinct agronomic advantages, including

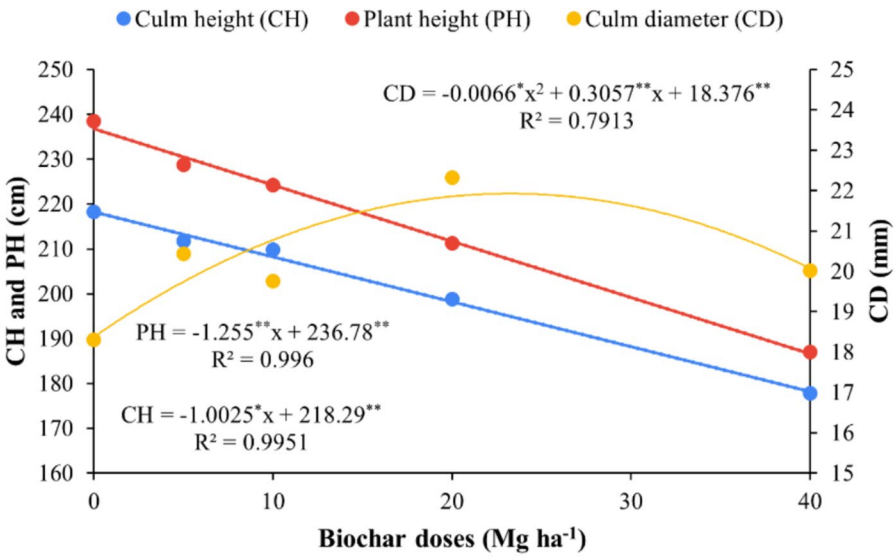

Fig. 9 Regressions for the growth parameters of culm height (CH), plant height (PH), and culm diameter (CD) related to biochar from sewage sludge added with cashew pruning. ** and * significant at 1% and 5% probability, respectively

enhanced resistance to lodging from strong winds and improved efficiency in both manual and mechanized harvesting (Losey et al. 2002; Stubbs et al. 2020). Additionally, the observed increase in culm diameter with SSPB treatment correlates with greater plant robustness and resilience against pest infestations (Zhao et al. 2022).

The temporal dynamics of biochar effects were highlighted by Cong et al. (2023), who documented an initial growth inhibition in maize following high-dose wheat straw biochar applications (63–126 Mg ha^{-1}) in sandy soils, attributed to elevated soil pH, electrical conductivity, and potential phytotoxic compounds. However, these inhibitory effects diminished over seven years, ultimately benefiting crop growth. Similarly, in this study, the reduction in plant height at higher SSPB doses (e.g., 40 Mg ha^{-1}) may be linked to trace heavy metals (Cd, Pb, Cr, Ni, Ba) and micronutrients (Mn, Fe, Mo, Zn) present in the biochar (Table 2), where the threshold between essentiality and toxicity is narrow. Notably, this height reduction did not reduce biomass, instead producing more compact, stress-resilient plants—a trait not inherently detrimental.

Another plausible factor is the sodium content in SSPB (4.09 g kg^{-1}; Table 2). Given maize's moderate sensitivity to salinity (threshold: 1.7 dS m^{-1} ≈ 1.088 g kg^{-1}; Ayers and Westcot 1999), elevated sodium levels could partially explain the stunted height and vegetative growth, depending on varietal tolerance and soil-specific conditions. Importantly, these phenotypic changes did not compromise biomass accumulation, underscoring the potential of SSPB to optimize plant architecture while maintaining productivity under controlled nutrient regimes. The findings align with broader evidence that biochar's benefits often emerge over time, balancing initial physicochemical constraints with long-term soil improvements.

4 Conclusions

Biochar derived from the co-pyrolysis of sewage sludge and cashew pruning residues significantly improves the physical quality of sandy soils more effectively than biochar from cashew bagasse. Key enhancements include reduced soil bulk density, increased aggregate stability, and optimized water retention, which are attributed to improved aggregate formation and modified porosity, facilitating efficient water use and robust root development. In contrast, cashew bagasse biochar primarily enhances water conservation during incubation but exhibits limited structural benefits.

The findings confirm three hypotheses: (1) both biochars enhance soil physical properties and maize growth, (2) the nutrient-rich sewage sludge and pruning biochar provides superior morphometric advantages for maize, and (3) optimal application rates differ between biochars—20–25 Mg ha^{-1} for the sludge-pruning blend and ~9 Mg ha^{-1} for bagasse.

From an economic standpoint, these biochar amendments offer substantial cost–benefit advantages. The enhanced soil structure and improved water dynamics can lead to reduced irrigation requirements and lower expenditures on additional soil amendments or chemical inputs. Moreover, the long-term benefits associated with restored soil health, including potential yield improvements and reduced management costs, underscore the economic viability of adopting biochar as a soil amendment.

These results elucidate the mechanistic links between biochar amendments, soil physical processes, and crop performance, offering practical strategies for recuperating degraded arid soils. The study establishes a framework for scaling sustainable land management in water-limited ecosystems. Future research should focus on long-term field trials, expanding the range of biochar doses, integrating biochar properties with plant–soil interactions, and assessing the economic feasibility of large-scale deployment.

Supplementary Information The online version contains supplementary material available at https://doi.org/10.1007/s42729-025-02509-6.

Acknowledgements We thank the Coordination for the Improvement of Higher Education Personnel (CAPES) for financial support (Code 001), the Funding Authority for Studies and Projects (FINEP) for financial support (Process nº 0122017200), the Ceará State Water and Sewerage Company (CAGECE) and the Ceará Foundation for Scientific and Technological Development Support (FUNCAP) for financial support (Process 06670855/2021), the Chief Scientist Program in Agriculture of the Government of the State of Ceará for financial support (Agreement 14/2022 SDE/ADECE/FUNCAP, Process 08126425/2020/FUNCAP) and INCTAgriS for financial support (Process 406570/2022-1). J.M.R.S is grateful to FUNCAP for the scholarship grant under Process No. BMD-0008-01029.01.08/23. Jaedson C.A. Mota, Mirian C. G. Costa, and Carlos T. S. Dias thank CNPq for the research grants (Processes nº 303524/2022-7, 305907/2019-0, and 303810/2023-8, respectively). Odair P. Ferreira also thanks the National Council for Scientific and Technological Development (CNPq) for financial support (grant numbers: 409205/2023-0 and 310821/2022-3).

Data Availability The data supporting this study's findings are available from the corresponding author upon reasonable request.

Declarations

Conflict of interest The authors declare that they have no financial or personal relationships that could have impacted on the work presented in this paper.

References

Ali O, Cheddadi I, Landrein B, Long Y (2023) Revisiting the relationship between turgor pressure and plant cell growth. New Phytol 238:62–69. https://doi.org/10.1111/nph.18683

Ayers RS, Westcot DW (1999) A qualidade da água na agricultura (Language: Portuguese). UFPB, Campina Grande.

Barbosa FLA, Santos JMR, Mota JCA, Costa MCG, Araujo ASF, Garcia KGV, Almeida MS, Nascimento IV, Medeiros EV, Ferreira OP, Souza Filho AG, Fregolente LG, Sousa HHF, Borges WL, Pereira APA (2024) Potential of biochar to restoration of microbial biomass and enzymatic activity in a highly degrade semiarid soil. Scientific Reports 14:26065. https://doi.org/10.1038/s41598-024-77368-9

Bekchanova M, Campion L, Bruns S, Kuppens T, Lehmann J, Jozefczak M, Cuypers A, Malina R (2024) Biochar improves the nutrient cycle in sandy-textured soils and increases crop yield: a systematic review. Environ Evid 13:3. https://doi.org/10.1186/s13750-024-00326-5

Blake GR, Hartge KH (1986) Particle Density. In: Klute A (ed) Methods of Soil Analysis: Part 1 Physical and Mineralogical Methods. Soil Science Society of America, Madison, pp 363–375. https://doi.org/10.2136/sssabookser5.1.2ed.c14

Blake GR, Hartge KH (1986) Bulk Density. In: Klute A (ed) Methods of Soil Analysis: Part 1 Physical and Mineralogical Methods. Soil Science Society of America, Madison, pp 363–375. https://doi.org/10.2136/sssabookser5.1.2ed.c13

Blanco-Canqui H (2017) Biochar and Soil Physical Properties. Soil Sci Soc Am J 81:687–711. https://doi.org/10.2136/sssaj2017.01.0017

Box GEP, Cox DR (1964) An Analysis of Transformations. J R Stat Soc Ser B (Methodol) 26:211–243. https://doi.org/10.1111/j.2517-6161.1964.tb00553.x

Bronick CJ, Lal R (2005) Soil structure and management: A review. Geoderma 124:3–22. https://doi.org/10.1016/j.geoderma.2004.03.005

Busscher WJ, Novak JM, Evans DE, Watts DW, Niandou MAS, Ahmedna M (2010) Influence of pecan biochar on physical properties of a Norfolk loamy sand. Soil Sci 175:10–14. https://doi.org/10.1097/SS.0b013e3181cb7f46

Cao J, Jiang Y, Tan X, Li L, Cao S, Dou J, Chen R, Hu X, Qiu Z, Li M, Chen Z, Zhu H (2024) Sludge-based biochar preparation: Pyrolysis and co-pyrolysis methods, improvements, and environmental applications. Fuel 373:132265. https://doi.org/10.1016/j.fuel.2024.132265

Chen C, Wang R, Shang J, Liu K, Irshad MK, Hu K, Arthur E (2018) Effect of biochar application on hydraulic properties of sandy soil under dry and wet conditions. Vadose Zone J 17:1–8. https://doi.org/10.2136/vzj2018.05.0101

Chen X, Liu L, Yang Q, Xu H, Shen G, Chen Q (2024) Optimizing biochar application rates to improve soil properties and crop growth in saline-alkali soil. Sustainability 16:6. https://doi.org/10.3390/su16062523

Cong M, Hu Y, Sun X, Yan H, Yu G, Tang G, Chen S, Xu W, Jia H (2023) Long-term effects of biochar application on the growth and physiological characteristics of maize. Front Plant Sci 14:1172425. https://doi.org/10.3389/fpls.2023.1172425

Costa A, De Freitas Neto AH, Szimsek C, Murara H G, Lehmkuhl L (2022) Atributos físicos e químicos do solo e produção de milho e soja em função da aplicação de condicionador de solo (Language: Portuguese) (Physical and chemical attributes of soil and corn and soybean production as a function of soil conditioner application). Agropecuária Catarinense 35:79–84. https://doi.org/10.52945/rac.v35i1.1117

Dexter AR, Kroesbergen B (1985) Methodology for determination of tensile strength of soil aggregates. J Agric Eng Res 31:139–147. https://doi.org/10.1016/0021-8634(85)90066-6

Dourado Neto D, Nielsen DR, Hopmans JW, Reichardt K, Bacchi OOS, Lopes PP (2001) Programa para confecção da curva de retenção de água no solo, modelo van Genuchten (Language: Portuguese) (Program for creating the soil water retention curve, van Genuchten model). Soil Water Retention Curve, SWRC (version 3.0 beta). Piracicaba, Universidade de São Paulo

Edeh IG, Mašek O, Buss W (2020) A meta-analysis on biochar's effects on soil water properties–New insights and future research challenges. Sci Total Environ 714:136857. https://doi.org/10.1016/j.scitotenv.2020.136857

Eibisch N, Durner W, Bechtold M, Fuß R, Mikutta R, Woche SK, Helfrich M (2015) Does water repellency of pyrochars and hydrochars counter their positive effects on soil hydraulic properties? Geoderma 245–246:31–39. https://doi.org/10.1016/j.geoderma.2015.01.009

Enders A, Lehmann J (2012) Comparison of wet-digestion and dry-ashing methods for total elemental analysis of biochar. Commun Soil Sci Plant Anal 43:1042–1052. https://doi.org/10.1080/00103624.2012.656167

Fakayode OA, Aboagarib EAA, Zhou C, Ma H (2020) Co-pyrolysis of lignocellulosic and macroalgae biomasses for the production of biochar–a review. Biores Technol 297:122408. https://doi.org/10.1016/j.biortech.2019.122408

Fernandes VLB (1993) Recomendações de adubação e calagem para o estado do Ceará (Language: Portuguese) (Fertilization and liming recommendations for the state of Ceará). Universidade Federal do Ceará, Fortaleza

Fregolente LG, Rodrigues MT, Oliveira NC, Araújo BS, Nascimento ÍV, Souza Filho AG, Paula AJ, Costa MCG, Mota JCA, Ferreira OP (2023) Effects of chemical aging on carbonaceous materials: Stability of water-dispersible colloids and their influence on the aggregation of natural-soil colloid. Sci Total Environ 903:166835. https://doi.org/10.1016/j.scitotenv.2023.166835

Garg A, Bordoloi S, Ni J, Cai W, Maddibiona PG, Mei G, Poulsen TG, Lin P (2019) Influence of biochar addition on gas permeability in unsaturated soil. Geotechnique Letters 9:66–71. https://doi.org/10.1680/jgele.18.00190

Gee GW, Bauder JW (1986) Particle size analysis. In: Klute A (ed) Methods of Soil Analysis. Agron Monger, Madison, pp 388–409

Goldan E, Nedeff V, Barsan N, Culea M, Tomozei C, Panainte-Lehadus M, Mosnegutu E (2022) Evaluation of the use of sewage sludge biochar as a soil amendment-a review. Sustainability 14:9. https://doi.org/10.3390/su14095309

Haghnia GH, Pratt PF (1988) Effect of exchangeable magnesium on the accumulation of sodium and potassium in soils. Soil Sci 145:432436. https://doi.org/10.1097/00010694-198806000-00005

International Biochar Initiative (2015) Standardized product definition and product testing guidelines for biochar that is used in soil. Int Biochar Initiat 23. https://doi.org/10.1016/j.zefq.2013.07.002.

IUSS Working Group WRB (2022) World Reference Base for Soil Resources. International soil classification system for naming soils and creating legends for soil maps. Vienna, Austria.

Jorge RF, Corá JE, Barbosa JC (2010) Número mínimo de tensões para determinação da curva característica de retenção de água de um Latossolo Vermelho eutrófico sob sistema de semeadura direta (Language: Portuguese). Rev Bras Ciênc Solo 34:1831–1840. https://doi.org/10.1590/S0100-06832010000600007

Junior A, Guo M (2023) Efficacy of sewage sludge derived biochar on enhancing soil health and crop productivity in strongly acidic soil. Front Soil Sci 3:1066547. https://doi.org/10.3389/fsoil.2023.1066547

Kemper WD, Rosenau RC (1986) Aggregate stability and size distribution. In: Klute A (ed) Methods of Soil Analysis. Madison (WI), ASA and SSSA, pp 425–442

Kiehl EJ (1979) Manual de Edafologia: relações solo-planta (Language: Portuguese). Agronômica Ceres, Piracicaba, SP.

Kimball BA, Boote KJ, Hatfield JL, Ahuja LR, Stöckle CO, Sotirios ABC, Basso B, Bertuzzi P, Constantin J, Deryng D, Dumont B, Durand JL, Ewert F, Gaiser T, Gayler S, Hoffmann MP, Jiang Q, Kim SH, Lizaso J (2019) Simulation of maize evapotranspiration: An inter-comparison among 29 maize models. Agric for Meteorol 271:264–284. https://doi.org/10.1016/j.agrformet.2019.02.037

Kloss S, Zehetner F, Dellantonio A, Hamid R, Ottner F, Liedtke V, Schwanninger M, Gerzabek MH, Soja G (2012) Characterization of Slow Pyrolysis Biochars: Effects of Feedstocks and Pyrolysis Temperature on Biochar Properties. J Environ Qual 41:990–1000. https://doi.org/10.2134/jeq2011.0070

Koorneef GJ, Pulleman MM, Comans RN, van Rijssel SQ, Barré P, Baudin F, de Goede RG (2024) Assessing soil functioning: What is the added value of soil organic carbon quality measurements alongside total organic carbon content? Soil Biol Biochem 196:109507. https://doi.org/10.1016/j.soilbio.2024.109507

Kumar M, Xiong X, Wan Z, Sun Y, Tsang DCW, Gupta J, Gao B, Cao X, Tang J, Ok YS (2020) Ball milling as a mechanochemical technology for fabrication of novel biochar nanomaterials. Bioresour Technol 312:123613. https://doi.org/10.1016/j.biortech.2020.123613

Li Y, Han Yu, Liu L, Hongbing Yu (2021) Application of co-pyrolysis biochar for the adsorption and immobilization of heavy metals in contaminated environmental substrates. J Hazard Mater 420:126655. https://doi.org/10.1016/j.jhazmat.2021.126655

Li S, Wang B, Zhang X, Wang H, Yi Y, Huang X, Gao X, Zhu P, Han W (2023) Soil particle aggregation and aggregate stability associated with ion specificity and organic matter content. Geoderma 429:116285. https://doi.org/10.1016/j.geoderma.2022.116285

Lim TJ, Spokas KA, Feyereisen G, Novak JM (2016) Predicting the impact of biochar additions on soil hydraulic properties. Chemosphere 142:136–144. https://doi.org/10.1016/j.chemosphere.2015.06.069

Lima AYV, Cherubin MR, da Silva DF, Mota JCA, Silva FGM, de Araujo ASF, Melo VMM, Verma JP, Pereira APA (2024) Grazing exclusion restores soil health in Brazilian drylands under desertification process. Appl Soil Ecol 193:105107. https://doi.org/10.1016/j.apsoil.2023.105107

Logsdon SD (2012) Temporal variability of bulk density and soil water at selected field sites. Soil Sci 177(5):327–331. https://doi.org/10.1097/SS.0b013e31824d8db1

Losey JE, Carter ME, Silverman SA (2002) The effect of stem diameter on European corn borer behavior and survival: potential consequences for IRM in Bt-corn. Entomol Exp Appl 105:89–96. https://doi.org/10.1046/j.1570-7458.2002.01037.x

Major J (2010) Guidelines on practical aspects of biochar application to field soil in various soil management systems. International Biochar Initiative, United States. Disponível via https://www.biocharinternational.org/wpcontent/uploads/2018/04/IBI%20Biochar%20Application%20Guidelines_web.pdf

Nascimento ÍV, de Alencar TL, dos Santos CLA, de Júnior RNA, Mota JCA (2018a) Effect of sample re-saturation on soil-water characteristic curve. Revista Caatinga 31:446–454. https://doi.org/10.1590/1983-21252018v31n221rc

Nascimento ÍV, de Assis Júnior RN, Araújo JC, Alencar TL, Freire AG, Lobato MGR, Silva CP, Mota JCA, Nascimento CDV (2018b) Estimation of van Genuchten Equation Parameters in Laboratory and through Inverse Modeling with Hydrus-1D. J Agric Sci 10:102. https://doi.org/10.5539/jas.v10n3p102

Nascimento ÍV, Santos EB, Lopes AS, Queiroz S, Teixeira Filho CD, Romero RE, Costa MCG, Ferreira OP, Souza Filho AG, Fregolente LG, Silva FG, Pereira APA, Sousa HHF, Sobucki V, Reichert JM, Mota JCA (2024) Biochar from cashew residue enhances silicon adsorption and reduces cohesion and mechanical resistance at meso- and micro-structural scales of soil with cohesive character. Soil Tillage Res 241:106101. https://doi.org/10.1016/j.still.2024.106101

Oliveira LS, Maia RN, Assis Júnior RN, Romero RE, Costa MCG, Alencar TL, Mota JCA (2020) Tensile strength values for the degrees of soil consistency using human perception and TS-Soil device. Catena 190:104541. https://doi.org/10.1016/j.catena.2020.104541

Pacheco CAP, Parentoni SN, Guimaraes PDO, Gama E, Meirelles W, Ferreira ADS, Garcia J (2009) BRS 2022: híbrido duplo de milho. Embrapa Milho e Sorgo (Language: Portuguese), Brasília.

Reis DA, Lima CLR, Pauletto EA, Dupont PB, Pillon CN (2014) Tensile strength and friability of an Alfisol under agricultural management systems. Sci Agric 71:163–168. https://doi.org/10.1590/S0103-90162014000200012

Rui Z, Lu X, Li Z, Lin Z, Lu H, Zhang D, Shen S, Liu X, Zheng J, Drosos M, Cheng K, Bian R, Zhang X, Li L, Pan G (2022) Macroaggregates serve as micro-hotspots enriched with functional and networked microbial communities and enhanced under organic/inorganic fertilization in a paddy topsoil from southeastern China. Front Microbiol 13:831746. https://doi.org/10.3389/fmicb.2022.831746

Scotti C, Bertora C, Valagussa M, Borrelli L, Cabassi G, Tosca A (2022) Agroenvironmental Performances of Biochar Application in the Mineral and Organic Fertilization Strategies of a Maize- Ryegrass Forage System. Agriculture 12:7. https://doi.org/10.3390/agriculture12070925

Shah AN, Tanveer M, Shahzad B, Yang G, Fahad S, Ali S, Bukhari MA, Tung SA, Hafeez A, Souliyanonh B (2017) Soil compaction effects on soil health and cropproductivity: an overview. Environ Sci Pollut Res 24:10056–10067. https://doi.org/10.1007/s11356-017-8421-y

Silva AP, Kay BD, Perfect E (1994) Characterization of the Least Limiting Water Range of Soils. Soil Sci Soc Am J 58:1775–1781. https://doi.org/10.2136/sssaj1994.03615995005800060028x

Silva BF, Rodrigues RZS, Heiskanen J, Abera TA, Gasparetto SC, Biase AG, Ballester MVR, Moura YM, Piedade SMS, Silva AKO, Camargo PB (2023) Evaluating the temporal patterns of land use and precipitation under desertification in the semi-arid region of Brazil. Ecol Inform 77:102192. https://doi.org/10.1016/j.ecoinf.2023.102192

Six J, Paustian K, Elliott ET, Combrink C (2000) Soil Structure and Organic Matter: I. Distribution of Aggregate-Size Classes and Aggregate-Associated Carbon. Soil Sci Soc Am J 64:681–689. https://doi.org/10.2136/sssaj2000.642681x

Stavi I, Yizhaq H, Szitenberg A, Zaady E (2021) Patch-scale to hillslope-scale geodiversity alleviates susceptibility of dryland ecosystems to climate change: insights from the Israeli Negev. Curr Opin Environ Sustain 50:129–137. https://doi.org/10.1016/j.cosust.2021.03.009

Stubbs CJ, Seegmiller K, McMahan C, Sekhon RS, Robertson DJ (2020) Diverse maize hybrids are structurally inefficient at resisting wind induced bending forces that cause stalk lodging. Plant Methods 16:67. https://doi.org/10.1186/s13007-020-00608-2

Sun Z, Moldrup P, Elsgaard L, Arthur E, Bruun EW, Hauggaard-Nielsen H, De Jonge LW (2013) Direct and indirect short-term effects of biochar on physical characteristics of an arable sandy loam. Soil Sci 178:465–473. https://doi.org/10.1097/SS.0000000000000010

Tang Y, Liu X, Lian J, Cheng X, Wang GG, Zhang J (2023) Soil Depth Can Modify the Contribution of Root System Architecture to the

Root Decomposition Rate. Forests 14:1092. https://doi.org/10.3390/f14061092

Tanure MMC, da Costa LM, Huiz HA, Fernandes RBA, Cecon PR, Pereira Junior JD, da Luz JMR (2019) Soil water retention, physiological characteristics, and growth of maize plants in response to biochar application to soil. Soil Tillage Res 192:164–173. https://doi.org/10.1016/j.still.2019.05.007

Tormena CA, Silva AP, Libardi PL (1998) Caracterização do intervalo hídrico ótimo de um latossolo roxo sob plantio direto (Language: Portuguese). Rev Bras Cienc Solo 22:573–581. https://doi.org/10.1590/S0100-06831998000400002

Tormena CA, Fidalski J, Rossi Junior W (2008) Resistência tênsil e friabilidade de um Latossolo sob diferentes sistemas de uso (Language: Portuguese). Rev Bras Cienc Solo 32:33–42. https://doi.org/10.1590/S0100-06832008000100004

Van Bavel CHM (1950) Mean weight-diameter of soil aggregates as a statistical index of aggregation. Soil Sci Soc Am J 14:20–23. https://doi.org/10.2136/sssaj1950.036159950014000C0005x

van Genuchten MT (1980) A closed-form equation for predicting the conductivity of unsaturated soils. Soil Sci Soc Am J 44:892–897. https://doi.org/10.2136/sssaj1980.03615995004400050002x

van Lier QJ, Pinheiro EAR (2018) An alert regarding a common misinterpretation of the van genuchten α parameter. Rev Bras Cienc Solo 42:e0170343. https://doi.org/10.1590/18069657rbcs20170343

Verheijen FGA, Zhuravel A, Silva FC, Amaro A, Ben-Hur M, Keizer JJ (2019) The influence of biochar particle size and concentration on bulk density and maximum water holding capacity of sandy vs sandy loam soil in a column experiment. Geoderma 347:194–202. https://doi.org/10.1016/j.geoderma.2019.03.044

Wang X, He J, Bai M, Liu L, Gao S, Chen K, Zhuang H (2022) The Impact of Traffic-Induced Compaction on Soil Bulk Density, Soil Stress Distribution and Key Growth Indicators of Maize in North China Plain. Agriculture 12:8. https://doi.org/10.3390/agriculture12081220

Watts CW, Dexter AR (1998) Soil friability: theory, measurement and the effects of management and organic carbon content. Eur J Soil Sci 49:73–84. https://doi.org/10.1046/j.1365-2389.1998.00129.x

Wei B, Peng Y, Lin L, Zhang D, Ma L, Jiang L, Li Y, He T, Wang Z (2023) Drivers of biochar-mediated improvement of soil water retention capacity based on soil texture: A meta-analysis. Geoderma 437:116591. https://doi.org/10.1016/j.geoderma.2023.116591

Weil RR, Brady NC (2016) The nature and properties of soils. Pearson, Harlow.

Yang X, You X (2013) Estimating parameters of van Genuchten model for soil water retention curve by intelligent algorithms. Appl Math Inf Sci 7:1977–1983. https://doi.org/10.12785/amis/070537

Zanutel M, Garré S, Sanglier P, Bielders C (2024) Biochar modifies soil physical properties mostly through changes in soil structure rather than through its internal porosity. Vadose Zone Journal 23:e20301. https://doi.org/10.1002/vzj2.20301

Zhang Y, Yang J, Yao R, Wang X, Xie W (2020) Short-term effects of biochar and gypsum on soil hydraulic properties and sodicity in a saline-alkali soil. Pedosphere 30:694–702. https://doi.org/10.1016/S1002-0160(18)60051-7

Zhao H, Zhang D, Yang L, Cui T, Song W, He X, Wu H, Dong J (2022) Optimal Design and Experiment of Critical Components of Hand-Pushing Corn Plot Precision Planter. Agriculture 12:12. https://doi.org/10.3390/agriculture12122103

Zong Y, Chen D, Lu S (2014) Impact of biochars on swell–shrinkage behavior, mechanical strength, and surface cracking of clayey soil. J Plant Nutr Soil Sci 177:920–926. https://doi.org/10.1002/jpln.201300596

Zornoza R, Moreno-Barriga F, Acosta JA, Muñoz MA, Faz A (2016) Stability, nutrient availability and hydrophobicity of biochars derived from manure, crop residues, and municipal solid waste for their use as soil amendments. Chemosphere 144:122–130. https://doi.org/10.1016/j.chemosphere.2015.08.046

Zusevics JA (1980) Seasonal Changes of Permanent Wilting Coefficient In Some Selected Tropical Soil. Commun Soil Sci Plant Anal 11:843–850. https://doi.org/10.1080/00103628009367084